LAWRENCE
LIVERMORE
NATIONAL
LABORATORY

LLNL-TR-418046

LLNL Contribution to LLE FY09 Annual Report: NIC and HED Results

R. F. Heeter, O. L. Landen, W. W. Hsing, K. B. Fournier

October 14, 2009

Disclaimer

This work performed under the auspices of the U.S. Department of Energy by Lawrence Livermore National Laboratory under Contract DE-AC52-07NA27344.

FY09 LLNL OMEGA Experimental Programs

In FY09, LLNL led 238 target shots on the OMEGA Laser System. Approximately half of these LLNL-led shots supported the National Ignition Campaign (NIC). The remainder was dedicated to experiments for the high-energy-density stewardship experiments (HEDSE).

Objectives of the LLNL led NIC campaigns at OMEGA included:

- *Laser-plasma interaction studies in physical conditions relevant for the NIF ignition targets*
- *Demonstration of Tr = 100 eV foot symmetry tuning using a reemission sphere*
- *X-ray scattering in support of conductivity measurements of solid density Be plasmas*
- *Experiments to study the physical properties (thermal conductivity) of shocked fusion fuels*
- *High-resolution measurements of velocity nonuniformities created by microscopic perturbations in NIF ablator materials*
- *Development of a novel Compton Radiography diagnostic platform for ICF experiments*
- *Precision validation of the equation of state for quartz.*

The LLNL HEDSE campaigns included the following experiments:

- *Quasi-isentropic (ICE) drive used to study material properties such as strength, equation of state, phase, and phase-transition kinetics under high pressure*
- *Development of a high-energy backlighter for radiography in support of material strength experiments using Omega EP and the joint OMEGA-OMEGA-EP configuration*
- *Debris characterization from long-duration, point-apertured, point-projection x-ray backlighters* for NIF radiation transport experiments
- *Demonstration of ultrafast temperature and density measurements with x-ray Thomson scattering from short-pulse laser-heated matter.*
- *The development of an experimental platform to study nonlocal thermodynamic equilibrium (NLTE) physics using direct-drive implosions*
- *Opacity studies of high-temperature plasmas under LTE conditions*
- *Characterization of copper (Cu) foams for HEDSE experiments.*

This work performed under the auspices of the U.S. Department of Energy by Lawrence Livermore National Laboratory under Contract DE-AC52-07NA27344.

National Ignition Campaign

Laser-Plasma Interactions

The laser-plasma interaction experiments in FY09 continued to emulate the plasma conditions expected along the laser-beam path in inertial confinement fusion designs. An interaction beam (Beam 30) aligned along the axis of a gas-filled hohlraum is used to study laser beam propagation. This year, the effect of polarization smoothing was shown to increase laser SBS backscatter thresholds by about the 1.6x factor expected analytically and from simulations [1]. Second, the sensitivity of SRS to density was checked in NIC-relevant plasmas [2]. The results will be also be presented as an invited talk at the APS DPP 2009 meeting.

[1]. D. Froula et. al., Phys. Rev. Lett., **101** 115002 (2008)
[2]. D. Froula et. al., Phys. Rev. Lett., **103** 045006 (2009)

Symmetry Diagnosis by Reemission Sphere

The indirect-drive National Ignition Campaign (NIC) proposes to set the first 2 ns of hohlraum radiation symmetry by observing the instantaneous soft x-ray re-emission pattern from a high-Z sphere in place of the ignition capsule. The soft x-ray measurements require low-Z windows over diagnostic holes and the laser beams that otherwise would interact with these windows have to be turned off. To assess this technique under NIC conditions, we used the OMEGA Laser Facility to image the re-emission of Bi coated spheres placed inside a vacuum hohlraum with 200 ps-temporal, 50-100 μm-spatial and 30% spectral resolution. The experiment is shown schematically in Figure 1. Different from the previous experiments performed in scale 0.6 NIF hohlraums [1] the new experiments were performed in larger scale 0.93 NIF hohlraums. This allows hohlraum laser-entrance-hole size and inner laser-beam illumination, achieved by azimuthal steering of four inner beams away from the diagnostic window, that are similar to upcoming NIF experiments. Furthermore, compared to [1] these experiments use a less perturbing off-axis stalk rather than a thin CH tent to hold the capsule.

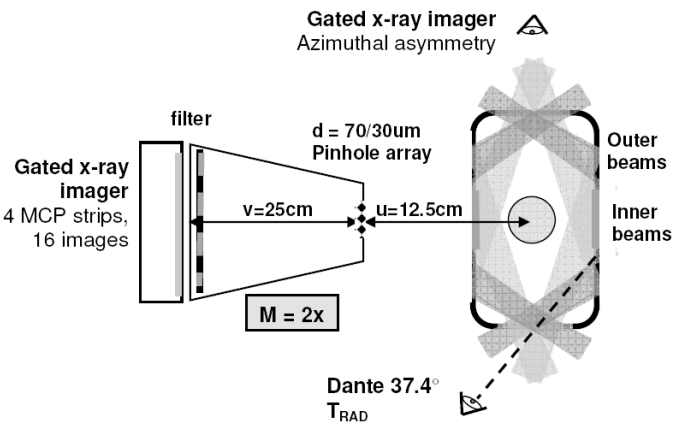

Figure 1: Re-emit experimental set-up for NIF and OMEGA.

As shown in Figure 2 by using 1 ns square laser pulses we achieved hohlraum radiation temperatures measured with Dante that are similar to those calculated for the future NIF experiments. The laser beams smoothed with SG4 phase plates generated intensities at the hohlraum wall that are similar to the foot of the NIF ignition design.

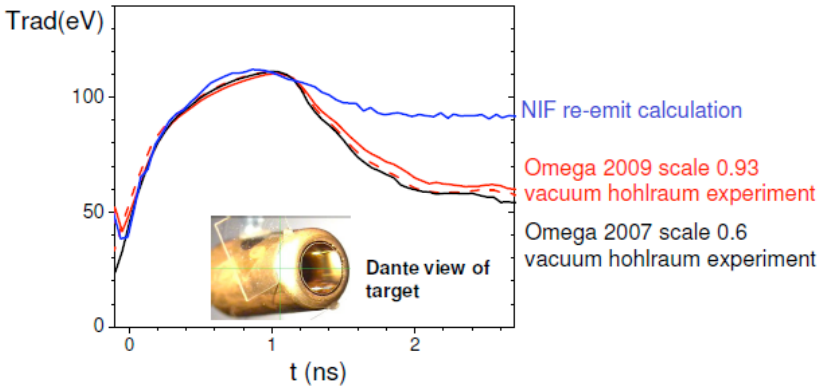

Figure 2: Hohlraum radiation temperatures measured with Dante in the OMEGA experiments and calculated for NIF.

We acquired good re-emit images in the 0.4-1.3 ns time interval corresponding to 85-115 eV NIF foot hohlraum temperatures for both 900 and 1200 eV energy bands at several inner-to-outer beam power balances; the images are shown in Figure 3. The x-ray background from the sphere stalk was negligible, validating the target design for the upcoming NIF re-emit experiments. The data confirms the required measurement accuracies of < 3% P_2/P_0 and P_4/P_0 Legendre mode flux asymmetry demonstrated in [1]. Furthermore, the image signal-to-noise is in agreement with a Planckian model for sphere re-emission, similar to [1].

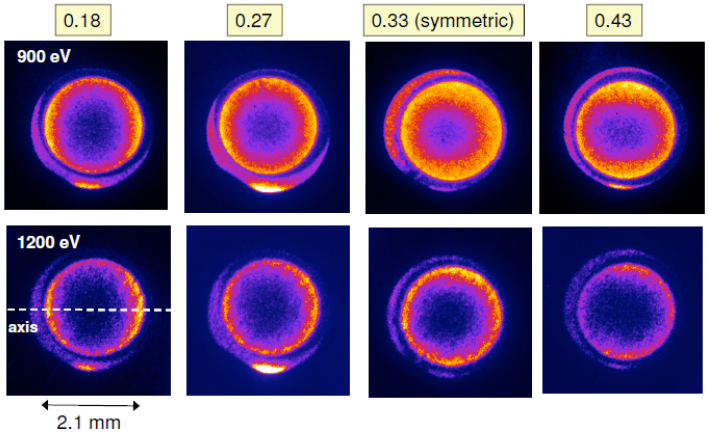

Figure 3: Re-emit images acquired at t=0.8 ns at 900 eV and 1200 eV energy bands versus inner-to-outer beam power balance (in units of inner/total laser power).

As shown in Figure 3, by changing the inner-to-outer beam power balance that will be used to tune early time P2/P0 in NIF ignition targets, we were able to change the radiation symmetry at the capsule from pole-hot to equator hot. Figure 4 shows the measured average P2/P0 as a function of power balance.

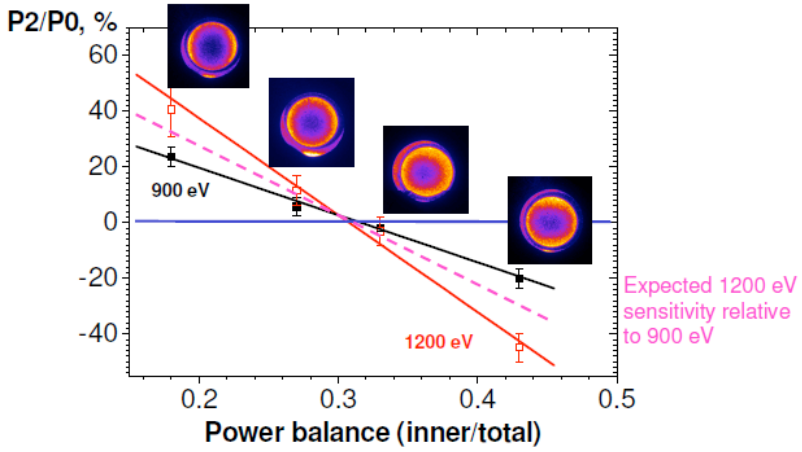

Figure 4: Re-emit images measured at 0.8 ns at 900 eV for constant and the corresponding P2/P0 versus inner-to-outer beam power balance

The measured P2/P0 sensitivity to power balance per beam is consistent with [1] where smaller hohlraums, larger LEH (75 vs 60% of the hohlraum diameter) and less inner beams (4 vs 8) were used. In both experiments the measured 1200 eV to 900 eV P2/P0 relative sensitivity of 2 is larger than the hν ratio (1.33) that is given by an ideal Planckian model for the sphere re-emission and this difference is under investigation.

[1] E.L. Dewald, C. Thomas, J. Milovich, J. Edwards, R. Kirkwood, D. Meeker, O. Jones, N. Izumi and O.L. Landen, *Rev. Sci. Instrum.* **79**, 10E903 2008

X-Ray Thomson Scattering – Conductivity of Warm, Dense Matter

The goal of these experiments in FY09 was to isochorically heat a 250 micron Be foil to sufficiently high temperatures that would allow to observe up-shifted plasmon signals with collective x-ray Thomson scattering (XRTS). Quantitatively measuring the ratio of up- over down-shifted plasmon strength enables to infer the electron plasma temperature based on first principles from the detailed balance relation, i.e. it is proportional to the Boltzmann factor $\exp(-h\nu_{res}/k_B T_e)$, with $h\nu_{res}$ the plasmon shift.

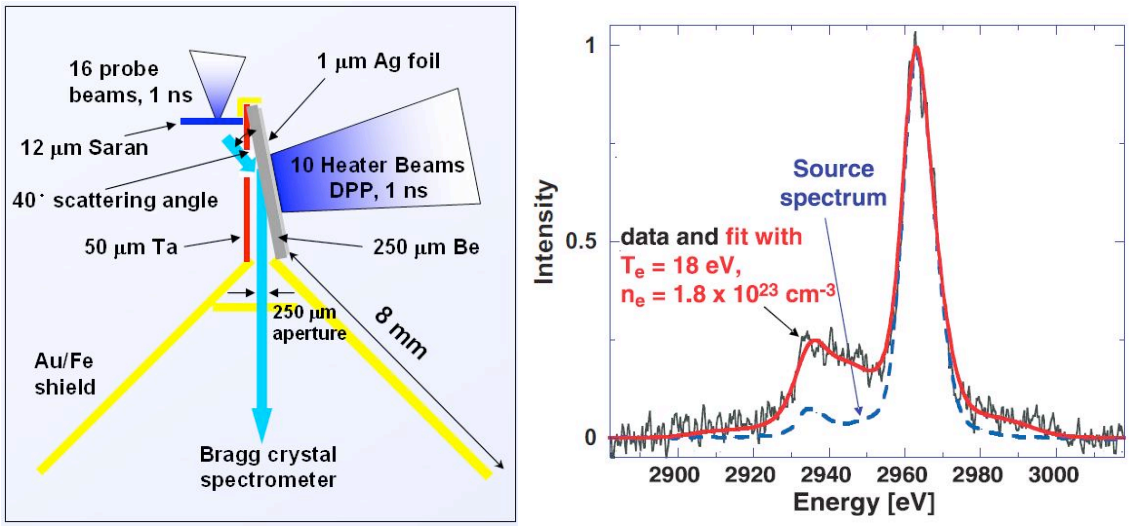

Figure 1: Left: Experimental setup to isochorically heat a 250 mm Be foil that is characterized with a Cl Ly-a x-ray probe at 2.96 keV. Shields block the direct line of sight to the spectrometer (towards the bottom). Right: X-ray Thomson scattering data show up- and down shifted plasmon signals that allow to infer temperature from detailed balance relation.

We utilized the XRTS target platform that had been proven very successful in experiments on shock-compressed Be. For isochoric heating we employed L-shell x-rays, that were created in thin Ag-, Au-, or Rh-foils that were directly mounted to the Be, cf. Fig. 1 for a schematic experimental setup. Time delayed to the 10 heater beams, 16 probe beams create the Cl Ly-alpha x-ray probe at 2.96 keV. The source spectrum is plotted on the right hand side of Fig. 1. The x-rays scattered off the rear Be surface under 40° scattering angle are recorded by the GTS spectrometer, which is based on HOPG as the Bragg crystal.

We obtained the best results with a silver x-ray converter foil. The scattering spectrum (black solid line), plotted on the right hand side of Fig. 1, shows inelastically scattered contributions that are up- and down-shifted in energy compared to the Cl Ly-alpha source line. The plasmon features are rather broad since the collectivity parameter $\alpha = 1.22$, putting the experiment just into the collective scattering regime. The best fit (red line) to the data is achieved for Te = 18 eV, and ne = 1.8e+23 cm^{-3}. The temperature is determined from detailed balance with an accuracy of 20%.

[1] Döppner *et al.,* HEDP **5**, 182 (2009)

[2] Döppner *et al.,* Proc. SPIE Vol. **7451** (2009).

D2 Thermal Conductivity

Reflectance and thermal conductivity of deuterium increase dramatically during compression above 1 Mbar. Simultaneous measurements of velocity, reflectance, and emissivity are being used to investigate the transport properties of cryogenic D_2 compressed by multiple shocks up to 6 Mbar at 7000 K (see Figure 1). Reliability improvements to the experimental platform will enable D_2 transport properties to be measured across a wide region of phase space in FY10.

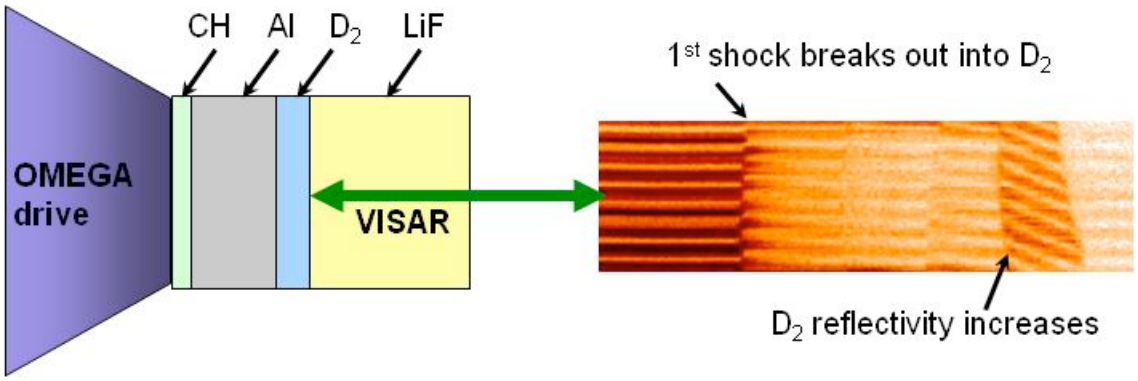

Figure 1: Experimental set-up and VISAR record of multi-shock compressed D_2 to 6 Mbar. A dramatic increase in the D_2 reflectance can be seen in the streak record at the arrival of the final shock.

Capsule Instability Seeding by Shock Non-Uniformity

Two consecutive shot days were devoted to CAPSEED campaigns in FY09. The primary focus of these campaigns was to study Be ablator samples of varying quality in order to compare with results from detailed metrology such as from grazing angle x-ray scattering, electron microscopy and surface profile measurements. The OHRV diagnostic was configured with higher sensitivity than previously in order to reduce the noise floor as low as possible. Analysis of the data led to several conclusions: (i) the velocity non-uniformities in high quality Be samples are effectively at the noise floor of the OHRV, which meets the NIF requirement for ablator performance; (ii) poor quality sample batches produced a higher level of non-uniformities than better quality. The velocity non-uniformities observed in the poor quality batches was attributed to the presence of a significant fraction of voids in the samples. The sample-quality is batch dependent, so it is possible to identify high- and low-quality batches after fabrication. This will help to eliminate low performing batches from the NIF experiments using electron microscopy and x-ray scattering. Future developments will focus on improving the noise floor of the instrument, and continuing with high sensitivity measurements on CH(Ge) and diamond samples.

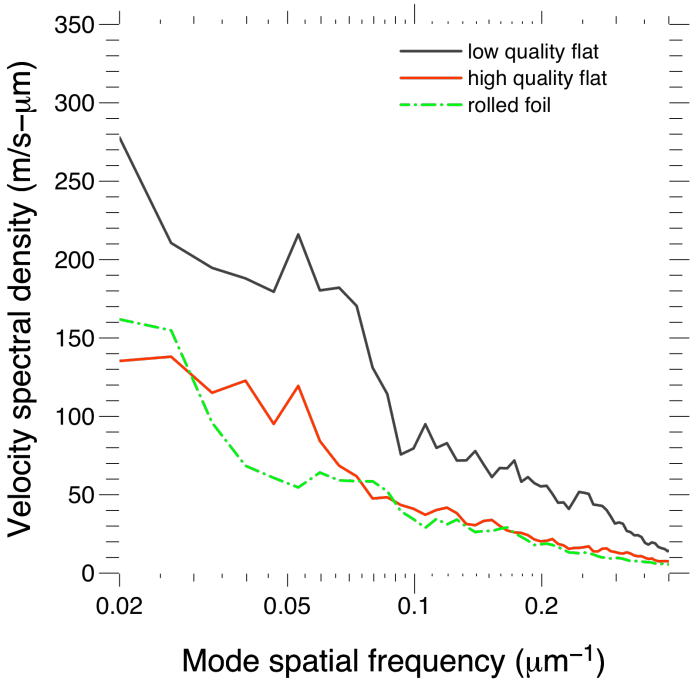

Figure 1: Velocity amplitude spectra recorded for three different Be sample types. The flats were Cu-doped sputtered Be foils, and the rolled foil was a polished sample of commercially available Be foil.

Compton Radiography

The goal of the Compton Radiography campaign is to build a novel diagnostic platform for ICF. In FY09 we successfully obtained the first ever radiographs of implosions, at photon energies around and above 60keV, where Compton scattering largely dominates the opacity of the plastic shell. In our experiments we used 60 beams of the OMEGA laser facility for direct-drive implosions of 40μm thick, 870μm diameter CH capsules filled with 3atm DD gas, located at the target chamber center of OMEGA. As a backlighter we used a 10μm diameter Au wire, 300 μm long, in a point-projection, end-on, geometry at 10mm distance from the CH shell. The backlighter was driven by the OMEGA EP short pulse beam, delivering ~1kJ at 10ps in a 100um square spot size. The time delay between the OMEGA EP short pulse and the OMEGA laser pulses was chosen to match the time of peak compression predicted by LILAC 1D simulations. In order to record the radiographs we designed and built a dedicated Compton Radiography Snout (CRS) consisting of a three-stage collimator, a layered structure of Al-Pb to shield against neutrons and high energy x and gamma rays, and a permanent magnetic field to deflect electrons away from the radiography lone of sight. CRS allows the insertion of filters at different locations and hosts a Fuji BAS imaging plate detector at about 400mm from target chamber center. By progressively increasing filtration in the CRS, we obtained good quality radiographs (with SNR of a few at 2% contrast) at (average) photon energies of approximately 60keV, 80keV and 100keV. As an example, Fig.1 shows a radiograph of the imploding CH shell, near peak compression, at t=4ns, obtained at a photon energy of ~60keV. The diameter measured from the radiograph is 70um: very close to the value of 60um predicted by LILAC 1D simulations. The CRS features a built-in step wedge filter that allows the reconstruction of the backlighting Bremsstrahlung spectrum and therefore the measurement of the density from the

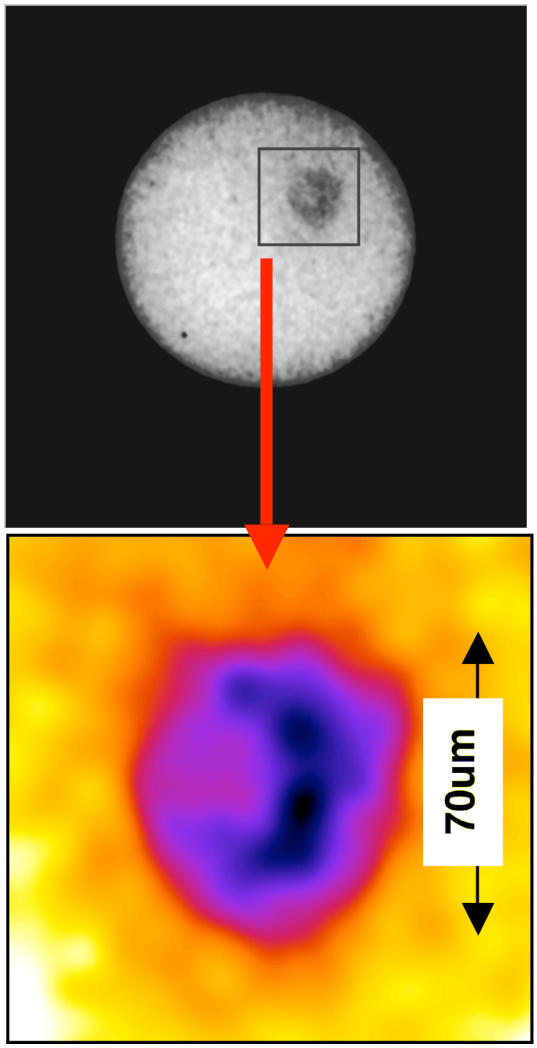

Fig.1: Compton Radiograph of CH shell near peak compression: <hν>~60keV. Upper picture shows CH shell radiograph inside shadow of CRS collimator. Lower picture shows blow-up of radiograph.

radiograph.

Precision Validation of Quartz Equation of State (EOS)

CH_n EOS measurements performed earlier in the year relied on the quartz as the impedance matching standard. The quartz (SiO_2) Hugoniot, measured several years ago at OMEGA, was found to be in good agreement with a linear shock velocity to particle velocity relation. This fit was also in agreement with earlier Russian measurements up to 6 Mbar and a single 20 Mbar point. However, given the sensitivity of impedance matching measurements to uncertainties in the impedance match standard, it was necessary to further improve our confidence in the quartz Hugoniot. This was done by using a new "boostrap" impedance matching method whereby quartz (ρ_0= 2.65 g/cc) is impedance matched to another polymorph of SiO_2 – fused silica (ρ_0= 2.2 g/cc). Since each Hugoniot probes a slightly different region of the SiO_2 high pressure phase diagram, the results are highly sensitive to derivative quantities, in particular the slope of the U_s-U_p relation and the Gruneisen parameter.

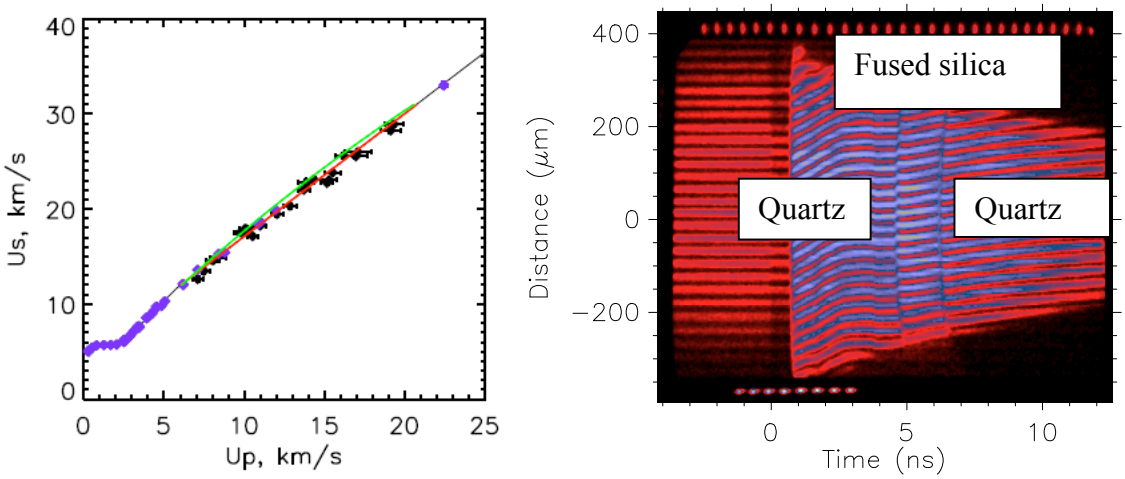

Figure 1: (a) Previously measured Quartz Hugoniot. The red line provides the best linear fit to data; the green line provides a possible, outlier fit to the data. New measurements were designed to determine possible deviations from the original linear fit. (b) Impedance matching of a quartz – fused silica – quartz target.

High-Energy-Density Stewardship Experiments

Material Properties

In FY09 5 experiment campaigns on OMEGA and OMEGA-EP were performed in support of the material dynamics effort: thin-walled hohlraum drive development (1/2 day each, 2 campaigns); low-density foam reservoir tests (1/2 day); tantalum Rayleigh-

Taylor experiment using OMEGA plus OMEGA-EP in a joint experiment day; and high-energy backlighter characterization (1 EP day).

Quasi-Isentropic Compression (ICE) Hohlraum Drive Development

The main goal of the first half-day of OMEGA shots was to test the thin-wall hohlraum performance to decrease the late-time Tr to delay and reduce the strength of the late-time shock in the quasi-isentropic pressure drive platform. The thin-wall hohlraums had a 1-micron Au wall with 100 micron thick Epoxy backing. The ablator was 75 μm of CH here to have a direct comparison with thick-walled hohlraum data from the previous March 2008. Our data suggest that the thin-wall hohlraums do delay the arrival of the late-time shock and we will be able to utilize this platform for our strength experiment. The other goal for this campaign was to test low density foams as the final layer in our reservoir. We tested 50 mg/cc SiO_2 aerogel (100 and 200 μm thick) and 100 mg/cc CRF (50 μm thick) foams. The ablator was 25 μm Be. Comparison between the data and the simulations showed that these low-density foams worked well and showed no hydro instabilities. The simulations of the VISAR data show abrupt velocity steps for each reservoir layer, corresponding to the foam followed by the CH(12.5% Br) layer. The data also showed distinct velocity steps for each reservoir layer, but the transition between layers was smoother than the simulated results, likely due to hydrodynamic mixing at the interface. Both simulations and data showed a late-time stagnation shock.

The goal of the second half day of OMEGA shots was to test the thin-walled hohlraum drive using both Al and Ta witness samples to verify that they give consistent drive measurements. These two witness plate samples gave consistent results. The second goal of this half-day was to test the stacked CRF foam reservoir properties: 50 μm of 500 mg/cc CRF followed by 100 μm of 50 mg/cc CRF. We used 25 μm Be ablators for all shots in this half day. This reservoir scales to a NIF design that reaches 5 Mb in a Ta strength experiment. Post-shot simulations match well with the measured drive using the stacked foam reservoir. The simulated VISAR results predicted abrupt velocity steps, corresponding to each layer in the reservoir. The data, however, showed much smoother transitions between the different layers in the reservoir, likely due to hydrodynamic mixing between the layers. Provided this mixing is reproducible, this added smoothing improves the drive by minimizing shock heating.

ICE Gradient-Density Reservoir Development

The goal of this half-day was to test the foam reservoir performance for the material strength experiment. Thus we used thick-walled hohlraums for this (since the foam in the reservoir modifies only the early-time drive). We tested the low density 50 mg/cc SiO_2 foams by measuring the shock-breakout (SBO) times from 75/100/125 microns of SiO_2 foam thicknesses. The data matched the predictions. The second part of the experiment was to test stacked foam layers in the reservoir of 500 mg/cc CRF (50 μm thick) and 50 mg/cc SiO_2 (100 μm thick). The release profile and the SBOs on various material layers were compared to simulations, with poor agreement between the detailed interface arrival times and shape. This could be due to uncertainties in the EOS of the SiO_2 foam.

ICE Tantalum Rayleigh-Taylor Experiments

We have successfully performed the first OMEGA and OMEGA-EP joint shots (60-beam long pulse plus EP short pulse lasers combined) to measure Ta Rayleigh-Taylor (RT) ripple growth to test models of Ta material strength at ~1 Mbar pressures and high strain rates, ~10^7 s^{-1}. The EP laser was utilized to generate a high-energy backlighter (> 20 keV) with high spatial resolution (<10 microns) to probe a 50-micron thick Ta sample with 3-micron peak-to-valley sinusoidal ripples. We had 4 joint shots to measure the Ta RT growth, interleaved with 6 OMEGA-only (long-pulse) shots to measure the hohlraum drive. The joint shot radiography technique worked well. For a couple of joints shots, the EP beam slightly missed the 100-μm-diameter micro-flat backlighter target, producing low-signal images. The growth factor measurements require a good understanding of the backlight spectrum. Fig. 1 shows the experimental configuration; Fig. 2 shows the target details and Fig. 3 shows a resulting Ta RT radiography image using the high energy Ag backlighter. Future experiments will acquire data that allows comparisons with predictions of Ta strength using standard material models (PTW, Steinberg-Guinan) at ~Mbar pressure. In conclusion, we have demonstrated that Rayleigh-Taylor experiments for Ta (and other high-Z) samples are possible and this type of experiment opens up a new capability for high-photon-energy radiography on Omega experiments. This experiment also led to 3 invited talks: IFSA 09 (The 6th international conference on Inertial Fusion Science and Applications, Sep, 2009, San Francisco); APS/DPP (American Physical Society, Nov. 2009, Atlanta); JOWG-37 (Oct, 2009, Livermore).

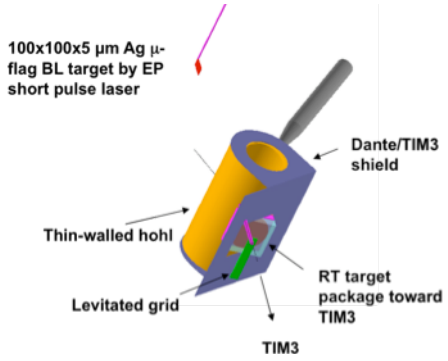

Fig. 1: ICETaRT-09A experimental setup

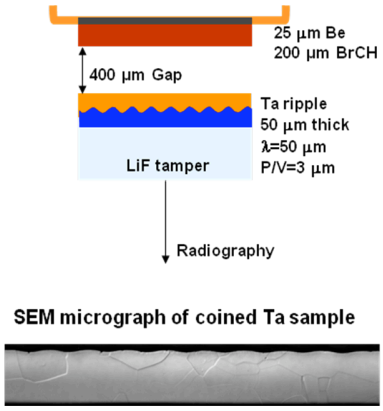

Fig. 2: ICETaRT target details

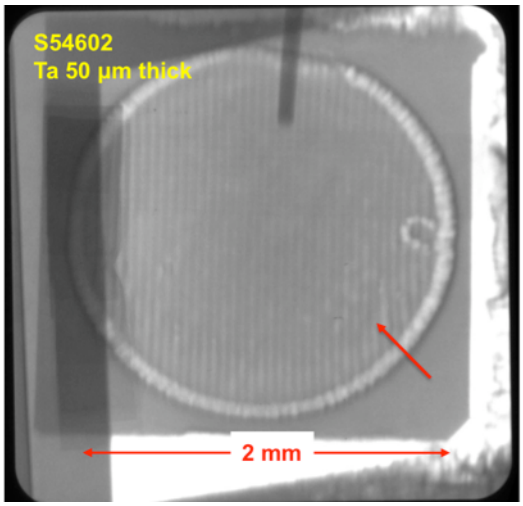

Fig. 3: ICETaRT radiography using OMEGA+EP joint shot

High-Energy Backlighter (HEBL) Development

The goal of the HEBL OMEGA-EP campaign was to measure the high-energy backlighter spectrum that would be utilized for the Ta Rayleigh-Taylor strength experiment on NIF. The high-energy backlighter is created by the OMEGA-EP short pulse beam illuminating a micro-flag target. The absolute spectrum will be crucial to the quantitative analysis of results from the radiography data. We utilized a transmission crystal spectrometer (TCS) that covers 15 to 70 keV range; Bremsstrahlung X-ray spectrometer (BMXS) that covers 70 keV to 1 MeV; and Ross-pair filters to get absolute yield in the 20 to 70 keV range. We had 6 shots total and our settings were changed to test: backlighter repeatability, laser spot size dependency, and radiography object dependency. By combining detectors that span different energy ranges we were be able to produce a composite spectrum from 15 keV to 1 MeV, as shown in Fig. 4.

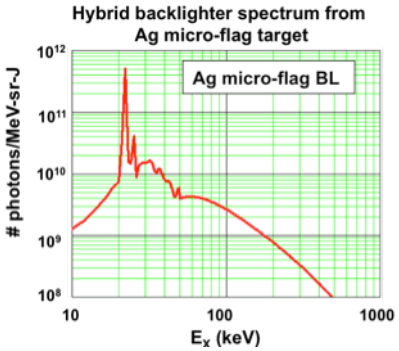

Fig 4. High-energy backlighter spectrum using EP short pulse laser. Measurements are made using many different detectors.

Debris Characterization from Long-Duration Point-Backlighters

An 8-nsec point-source backlighter developed on Omega was demonstrated on NIF for streaked radiography. This configuration provided sufficient photons, high spatial resolution (~ 20 μm) and instrument protection from debris. To extend this to multi-frame 2D radiography, experiments were performed on Omega to characterize the debris and signal level. Pinhole-apertured point-projection backlighters generally produce either solid or liquid ballistic spall from the pinhole substrate, which generally is accelerated normal to the pinhole surface. On experiments where using a tilted pinhole substrate is undesirable, diagnostics must be protected from spall launched directly at the x-ray detector. This is traditionally done with thick pieces of beryllium, which can offer protection without sacrificing x-ray transmission.

Alternate materials are being developed for debris mitigation for pinhole-apertured point-projection backlighters that are pointed directly at imaging diagnostics. We tested several thicknesses of aluminum and boron carbide (B_4C) for debris mitigation. Twenty OMEGA beams (10 kJ laser energy) drove a Ni pinhole-apertured point-projection backlighter (75 μm thick Ta pinhole substrate) from P6 towards up to six 75 μm-thick or up to three 150 μm-thick filters. These filters were spaced at least 15 mm apart in the MSpec snout in TIM 6, with an image plate in the SPCA detector. We found that three 150 μm-thick B4C filters encapsulated in 8 μm Kapton allowed 1-2 debris penetrations of the rear-most filter,, whereas three 75 μm-thick Al filters or two 150 μm-thick Al filters stopped all the ballistic debris, leaving at least 1 clean rear filter. This suggests that the debris can be mitigated while allowing sufficient X-ray transmission.

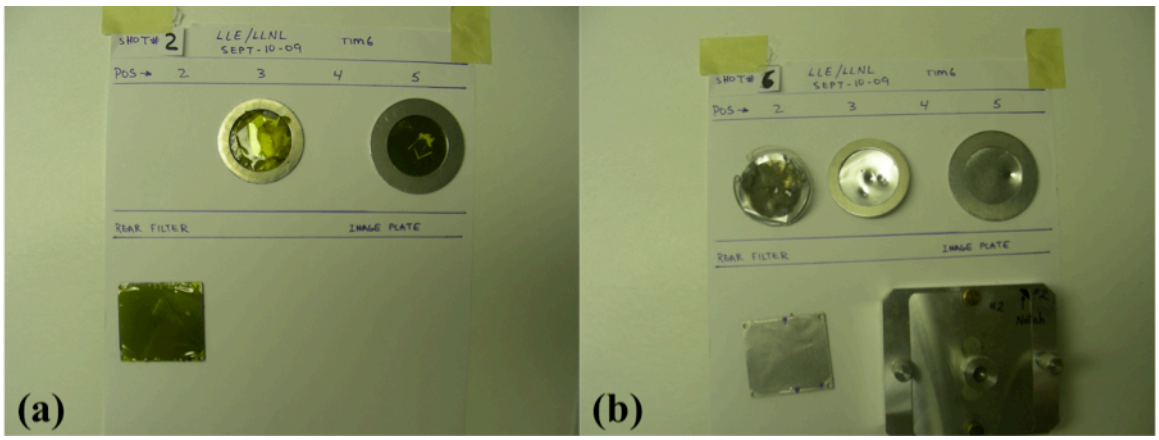

Figure 1: Damaged filters from debris testing. a) Three 150 μm-thick B4C-Kapton filters, showing one pinhole in the rear filter. b) Four 75 μm-thick Al filters, with the first three showing some ballistic damage, and a clean rear filter.

X-Ray Thomson Scattering

The objective of this campaign was to demonstrate ultrafast temperature and density measurements with x-ray Thomson scattering from short-pulse laser heated matter. In March 2009, we have applied the OMEGA-EP facility to heat a 200 μm beryllium cube with a 1 kJ, 10 ps short pulse laser beam, and have performed the first non-collective x-ray scattering measurements using a Zn Kα x-ray probe at 8.6 keV. The latter has been produced by the second OMEGA-EP 10 ps short pulse laser beam. On the first day of shots, we have performed a total of 4 shots among those have been the very first shots with two short pulse beams fired simultaneously for target physics experiments. In addition, we have successfully fielded the new Zink von Hamos (ZVH) high efficiency x-ray spectrometer, a dedicated diagnostic developed for the Kα x-ray Thomson scattering project. This instrument has shown the elastic and inelastic scattering signals of beryllium with only 180 J in the probe beam.

Since these experiments have used for the first time both OMEGA-EP short-pulse laser beams simultaneously on target, we had to field dedicated diagnostics to measure beam synchronization. At this point, we have achieved synchronization to an accuracy of only 250 ± 200 ps, which we will need to improve in the future to reach about 100 ps for this experiment. We have also employed low-energy activation shots (50 J) to successfully record the x-ray source spectrum and to determine the spectrometer dispersion. The third shot of the day has delivered ~1 kJ within a 10 ps pulse in the *backlighter* beam to heat the Be, and ~1.3 kJ in the *sidelighter* beam to create the x-ray probe. Since the sidelighter shot had been higher in energy than originally anticipated, we reduced the energy to 180 J on the last shot of the day. Nevertheless we have been able to record elastic and inelastic scattering signals of cold beryllium. This is a very promising result. We have also assessed the bremsstrahlung level and background levels. These measurements will enable us to improve the experimental design to measure

plasma temperatures of short pulse laser heated beryllium with high temporal resolution using Kα x-ray Thomson scattering on the next day of shots.

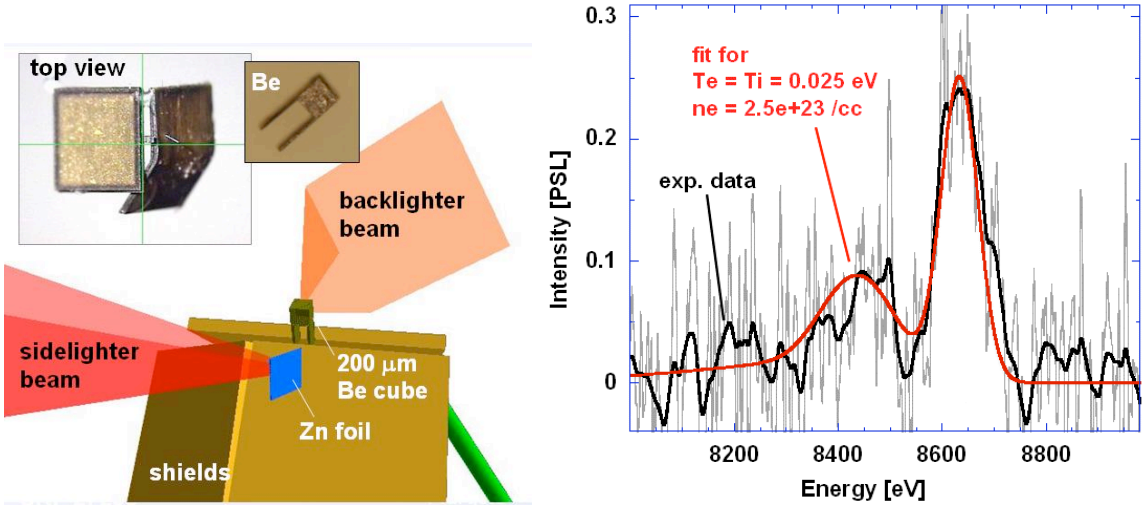

Figure 1: Left: Experimental setup showing the EP backlighter beam heating a 200 μm Be cube. The EP sidelighter beam creates the Zn Ka x-ray probe at 8.62 keV. Shields block the direct line of sight to the spectrometer (towards the bottom). Right: X-ray Thomson scattering spectrum from cold beryllium, measured with only 180 J in OMEGAEP sidelighter beam. The downshifted inelastically scattered Compton feature is fitted with the parameters for cold solid beryllium.

Non-LTE Implosions

The goal of the non-local thermodynamic equilibrium (NLTE) campaign is to build a platform to study the energy balance in implosions by measuring ion, electron, and radiation temperatures as a function of high-Z dopant concentration. In our experiments in FY09, we used 60 beams of the OMEGA laser facility for direct-drive implosions of thin (4 μm) glass capsules filled with 10 atm. D3He gas and Kr gas as a spectroscopic tracer. The relative concentration of DD and 3He was varied during the shots, the Kr concentrations were 0.001 and 0.005 atm. and some capsules also contained as much as ~ 0.1 atm. Xe. As a time resolved electron temperature (T_e) diagnostic, we fielded a mica conical crystal spectrometer that was coupled to a streak camera and viewed K-shell emission lines from the Kr dopant. Time integrated spectra were also recorded with the HENEX spectrometer. We also fielded a high-resolution spectrometer to use the Doppler broadening of x-ray lines for measuring T_i.

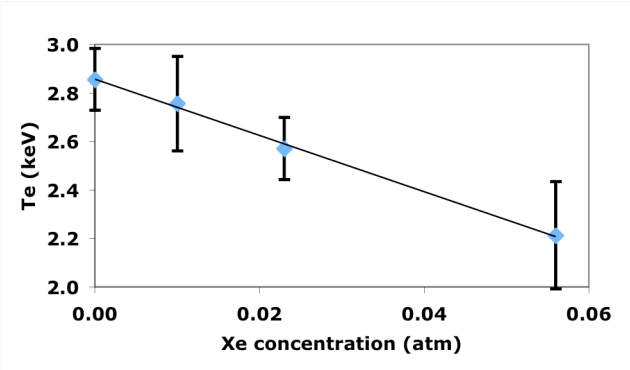

Figure 1: time integrated T_e , inferred from HENEX spectra, shows a linear decrease with increase of Xe dopant concentration.

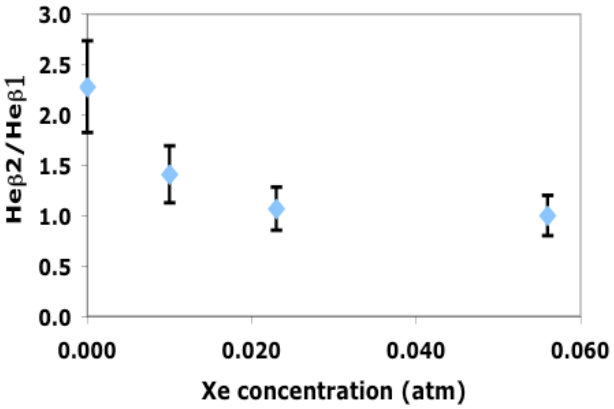

Figure 2: The He-β2/ He-β1 line ratio, measured from conical crystal spectra, shows decrease with increasing Xe concentration.

We observed a decrease of the DD/DT yield ratio with increasing Xe concentration. This trend is well reproduced by Lasnex/DCA:T simulations. We observed an increase of the DD/DT yield ratio with increasing DD concentration as well as an increase in the ion temperature, inferred from proton and neutron emission time histories and spectra. Increasing Xe dopant concentration appears to reduce compression-phase T_i by coupling to radiative cooling.

We inferred time integrated T_e from a Bremsstrahlung functional form fit to the continuum part of the spectra recorded by HENEX. As reported in Fig.1, Te shows a linear decrease with increase of Xe dopant concentration: a behavior reproduced by simulations, although experimental measurements give values higher by a factor of about

30%.

We used the time resolved spectra from the conical crystal spectrometer to study the temporal evolution of the Kr He-ß lines. The He-ß2/ He-ß1 line ratio shows a peak in the central 50ps of the Kr emission. The He-ß2/ He-ß1 line ratio also shows decrease with increasing Xe concentration, as reported on Fig. 2.

High-Temperature Plasma Opacity

In FY08 LLNL completed the development of a high-temperature laser opacity platform. In FY09, detailed X-ray transmission spectra from fully characterized, high temperature plasmas have been produced using the OMEGA laser, to provide validation benchmarks for the x-ray opacity codes (and associated data tables) underlying simulations of radiation transport experiments. Shots in FY09 produced detailed benchmark data on tantalum-titanium and sodium chloride-titanium plasmas. In these experiments, 24 beams heat a 1.6 mm diameter hohlraum, which in turn radiatively heats and expand a tamped Ti foil. Additional beams drive two broadband backlighters: a rear wall burnthrough halfraum (14 beams) and a Kr-filled "dynamic hohlraum" capsule implosion (10 beams). Looking through the sample to these backlighters, two broadband spectrometers characterize the sample transmission from 250-1600 eV and 3000-5500 eV, respectively; the lower energy band encompasses the bulk of the Rosseland Mean opacity. The plasma density of 0.05 ± 0.01 g/cc, measured by expansion radiography, agrees well with pre-shot calculations. The plasma temperature implied by the titanium ionization features in the 3000-5500 eV spectra is 110 ± 5 eV. Rosseland mean opacity data from 250-1600 eV is now being analyzed. Discrepancies with theory have been observed and are undergoing detailed investigation. For the future, an extension of these techniques to NIF would enable investigation of much hotter plasmas at conditions relevant to stellar core modeling, where recent observational data (helioseismology) contradicts standard solar models. A small change in the technique also enables a scaled experiment to study photoionized plasmas relevant to black hole accretion disk physics.

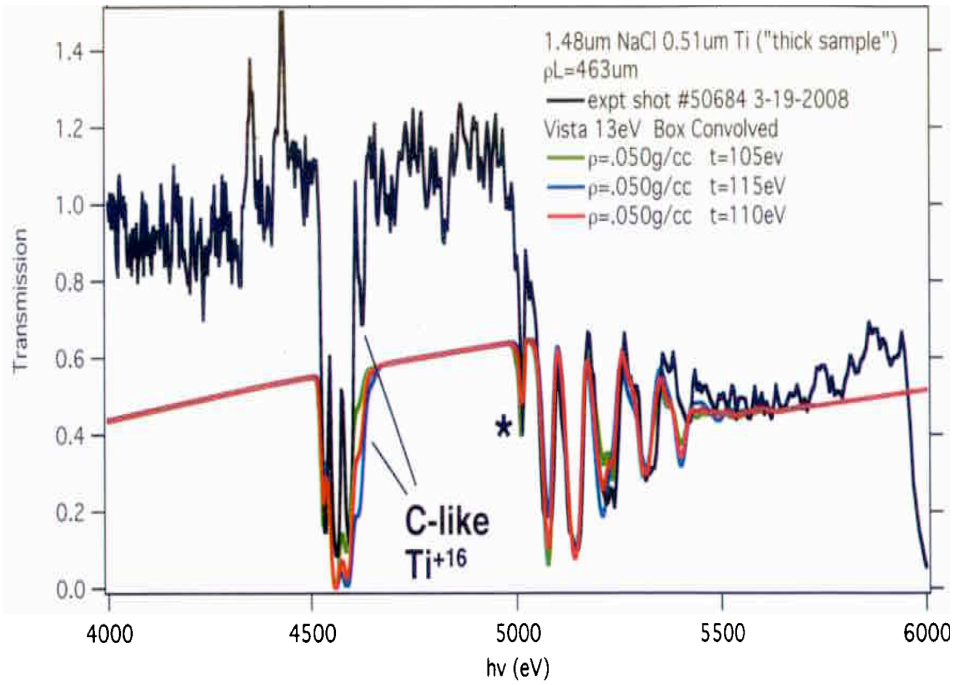

Figure 1: X-ray transmission opacity data from gated space-resolved titanium absorption spectra for photon energies from 4 to 5.9 keV. To the left are n=1 to 2 absorption lines of F-like to C-like Ti, with the C-like feature being strongly temperature-dependent. To the right are n=1 to 3 lines of the same ions, plus a narrow feature from the Ne-like ion (*). Analysis using the VISTA opacity model indicates a temperature of 110 ± 5 eV for densities in measured range, 0.050 ± 0.010 g/cc.

Characterization of Cu Foams

In support of characterization of Cu foams for HEDSE experiments, two half days (a total of eight shots) were fielded. Material characteristics of interest included both the internal energy (EOS) and the opacity of the foams, at several Mbar of pressure. Pure metal foams are of utility as backlighter sources, as low-density materials for radiation-hydrodynamic experiments and opacity experiments. The first set of shots used a hohlraum to drive a CH ablator paired with a Cu foam (density about 0.89 g/cm^3) and a SiO_2 payload (density 0.05 g/cc). The purpose of this experiment was to measure, on the same shot, shock breakout from the Cu into the (transparent) SiO_2, shock velocity in the SiO_2, and the position of the Cu/SiO_2 interface by point projection radiography. The results are sensitive to the EOS of the Cu foam, but not to the opacity. Post-shot simulations agreed with the experimental results. A typical radiograph from this series is shown on the left in the figure below.

The second round of shots continued characterization of Cu foam by using the Cu as an ablator in a hohlraum-driven experiment. The Cu ablator for a typical target is shown during the machining process (right image); the Cu foam density is about 0.89 g/cm^3. The

shock breakout time and the foil burn through time are sensitive to the opacity as well as the internal energy of the foam. The post-shot simulations again were consistent with the experimental results. The results allow the design of experiments using this Cu foam to go forward in FY10.

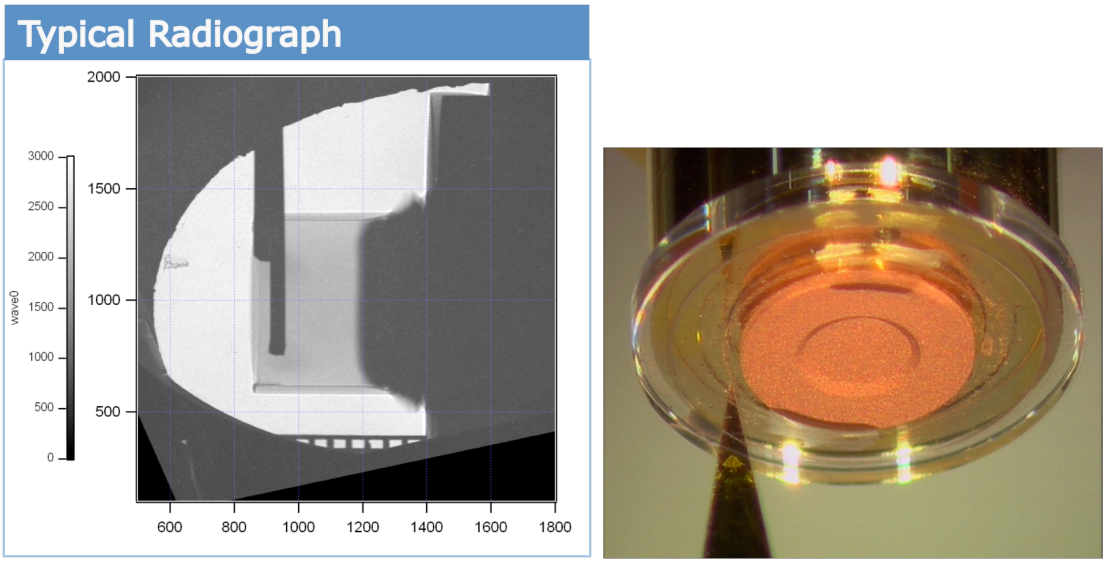

Figure 1: A typical radiograph taken during a shock-breakout experiment (left) and a picture of one of the copper foam ablator targets (right).